Table 2. Statistics of phasing. The figure of merit (mean value of the cosine of the phase angle error) is $\overline{M} = 0.77$ for this refinement, in which scale factors were refined for each reciprocal lattice level (that is, photograph) for the protein and derivative.

Derivative	RMS F_c,* electrons	RMS E,† electrons
Hg	476	216
Au	351	219
Pt	688	336
Ir	451	299

* Root mean square (RMS) $F_c = [\Sigma_j h^2/n]^{1/2}$, where f_{hj} is the heavy-atom scattering amplitude for reflection h of derivative j; n is the total number of reflections. The RMS structure factor of the native protein is 2870 electrons. † RMS $E = [\Sigma \epsilon_{hj}^2/n]^{1/2}$, where ϵ_{hj} is the lack of closure for reflection h of derivative j.

the regulatory region (Figs. 1 to 3). We see no conflict between our earlier maps (*8*) (or our present maps) and the electron micrographs obtained by Richards and Williams (*9*). We do not, however, fully agree with the interpretation (*10*) by Cohlberg *et al.* in which the R chains are represented by long rod-shaped "arms" 20 by 60 Å. We find that the regulatory dimer is more nearly globular in shape. The highly stained region within the molecule [figure 1 in (*9*)] which creates the appearance of "arms" can, in view of the x-ray results, be accounted for by (i) the accumulation of the stain in the central cavity and (ii) the relative thinness of stain-excluding protein in the R:C interface (see Fig. 4). Similarly, micrographs of the molecule viewed perpendicular to the threefold axis show a central dark staining region [figure 2 in (*9*)], which can now be interpreted as the central cavity.

One striking feature of the new map is the helix content, estimated as about 35 percent for the C unit and 10 percent for the R unit. Uncertainties in these numbers arise partly from the ambiguities in assigning the electron density in the region of contact between these units, and from lack of resolution of small helical regions.

A schematic drawing of the assembly of the two C_3 units and the regulatory units around the central cavity of aspartate transcarbamylase is shown in Fig. 1. This cavity has dimensions of about 25 Å along the threefold and about 50 Å along the three twofold axes (including both directions from the molecular center). A revision of the earlier interpretation is that the possible channel (*8*) along the threefold axis is now completely filled with protein density. The largest remaining channels to the central cavity are six openings, each 15 Å in diameter. These openings are

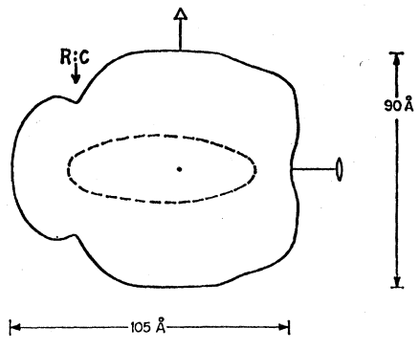

Fig. 4. Side view of the aspartate transcarbamylase molecule perpendicular to the threefold and one twofold axes, showing the central cavity and one regulatory dimer (left side). The boundary between regulatory and catalytic regions is suggested by the symbol R:C.

located near the median plane of the molecule in the region containing predominately R chains but also portions of the C chain.

Reaction of aspartate transcarbamylase with 2-chloromercuri-4-nitrophenol results in loss of enzyme activity, and does not dissociate the aspartate transcarbamylase molecule (*11*). It is likely that the thiol group which reacts with this mercurial is near the active site inasmuch as this derivative no longer binds succinate (*12*), although this thiol is not directly involved in binding or catalysis (*13*). According to the density map, this Hg site is easily accessible from the central cavity, but probably not directly from the outside of the aspartate transcarbamylase molecule.

A number of conformational changes are implicated in the catalytic and regulatory activities of aspartate transcarbamylase. An appealing possibility, suggested by our x-ray structure study, is that access to the central cavity of this enzyme is regulated by its interaction with CTP (and with adenosine triphosphate) (*14*). Central cavities in enzyme complexes may simply arise as a consequence of packing protein subunits around positions of high symmetry, like the 32 position in aspartate transcarbamylase. Further studies of this enzyme and of its complexes with effectors are under way in order to elucidate these mechanisms at the level of atomic resolution.

D. R. Evans, S. G. Warren
B. F. P. Edwards, C. H. McMurray
P. H. Bethge, D. C. Wiley
W. N. Lipscomb

Department of Chemistry,
Harvard University,
Cambridge, Massachusetts 02138

References and Notes

1. M. E. Jones, L. Spector, F. Lipmann, *J. Amer. Chem. Soc.* **77**, 819 (1955); P. Reichard and G. Hanshoff, *Acta Chem. Scand.* **10**, 548 (1956).
2. R. A. Yates and A. B. Pardee, *J. Biol. Chem.* **221**, 757 (1956).
3. J. C. Gerhart and A. B. Pardee, *ibid.* **237**, 891 (1962).
4. ———, *Fed. Proc.* **23**, 727 (1964).
5. J. C. Gerhart and H. K. Schachman, *Biochemistry* **4**, 1054 (1965).
6. D. C. Wiley and W. N. Lipscomb, *Nature* **218**, 1119 (1968).
7. K. Weber, *ibid.*, p. 1118.
8. D. C. Wiley, D. R. Evans, S. G. Warren, C. H. McMurray, B. F. P. Edwards, W. A. Franks, W. N. Lipscomb, *Cold Spring Harbor Symp. Quant. Biol.* **36**, 285 (1971).
9. K. E. Richards and R. C. Williams, *Biochemistry* **11**, 3393 (1972).
10. J. A. Cohlberg, V. P. Pigiet, Jr., H. K. Schachman, *ibid.*, p. 3396.
11. D. R. Evans, C. H. McMurray, W. N. Lipscomb, *Proc. Nat. Acad. Sci. U.S.A.* **69**, 3638 (1972).
12. C. H. McMurray, D. R. Evans, B. D. Sykes, *Biochem. Biophys. Res. Commun.* **48**, 572 (1972).
13. T. C. Vanaman and G. R. Stark, *J. Biol. Chem.* **245**, 3565 (1970).
14. The relative positions of the zinc ions and the C-chain SH-groups have been determined in crystals (*6*) of the CTP-aspartate transcarbamylase complex. Each zinc ion is 24 A away from the nearest C-chain SH-group.
15. We thank the National Institutes of Health and the Guggenheim Foundation for support of this research. A preliminary account of this research was given at the third Enzyme Conference, at the University of California, Los Angeles, 27 to 29 December 1972.

15 January 1973

Sea Urchin Sperm-Egg Interactions Studied with the Scanning Electron Microscope

Abstract. *Scanning electron microscopy of the outer surface of sea urchin eggs sampled at intervals during the first 3 minutes after insemination reveals the detailed structural changes of the vitelline layer during its transformation into the fertilization membrane. A sperm attachment-detachment sequence is described for the large number of sperm which transitorily bind every egg during fertilization.*

After insemination of the eggs of the purple sea urchin, *Strongylocentrotus purpuratus*, there is a 25-second latent period before the first morphological response of the egg in fertilization is initiated (*1, 2*). This response is cortical granule breakdown, which begins at the site of successful sperm penetration and propagates around the egg in the next 20 to 30 seconds (*3*). During the latent

period, many sperm attach to the vitelline layer of the egg by a protease-sensitive bond (*2, 4*). Recent work from our laboratory shows that the number of sperm bound per egg increases progressively up to 25 seconds after sperm addition. At this time the cortical reaction is initiated and a progressive detachment of the excess sperm occurs over a time course approximately coincident with that of cortical granule breakdown (*2*) and the concomitant release of a protease from the cortical granules (*2, 5*).

This sperm attachment-detachment sequence can be observed with the light or electron microscope since the attachment is preserved by using standard fixation procedures. These initial phases of fertilization, being surface phenomena, make the scanning electron microscope (SEM) ideally suited for such an investigation. We are describing here the results of a SEM examination of the events following insemination. Pictured are the topography of the vitelline layer, the sequence of sperm attachment and detachment to this structure, and the subsequent transformation of this layer into the fertilization membrane. The mechanism of the block to polyspermy in sea urchin eggs is discussed in relationship to this sperm attachment-detachment sequence.

Gametes of *S. purpuratus* were shed by KCl injection and collected by standard procedures (*2, 3*). The eggs were dejellied by a 2-minute exposure to seawater at *p*H 5 and then washed with normal seawater. Fertilization was achieved by rapidly adding and mixing 1 ml of sperm suspension to 3 ml of egg suspension in a 50 ml beaker. Relatively high concentrations of sperm (3×10^8 per milliliter) were used in these experiments to illustrate more clearly what happens at standard sperm concentrations (10^6 to 10^7 per milliliter). Under these conditions more sperm bind to each egg than under normal conditions of insemination, but the pattern of attachment and detachment remains the same (*6*). To arrest sperm-egg interactions and simultaneously fix the eggs at the indicated times for observation in the SEM, a portion of the gametes was added to an equal volume of 4 percent glutaraldehyde in 35 percent seawater. This final fixative solution is slightly hypotonic (948 milliosmoles per liter as measured by freezing point depression) with respect to seawater (1016 milliosmoles per liter). The fixed gametes were dehydrated by using a graded series of ethanol concentrations and dried by the Freon–critical point method (*7*). The dried specimens were placed on a rotary device, coated with a mixture of gold and palladium (60:40), and viewed in the Stereoscan S4 SEM (Cambridge Scientific Instruments, Ltd.). For observations by light microscopy, gametes were fixed by adding a portion to an equal volume of 15 percent formaldehyde in seawater, and viewed directly. All steps were performed at room temperature (22°C).

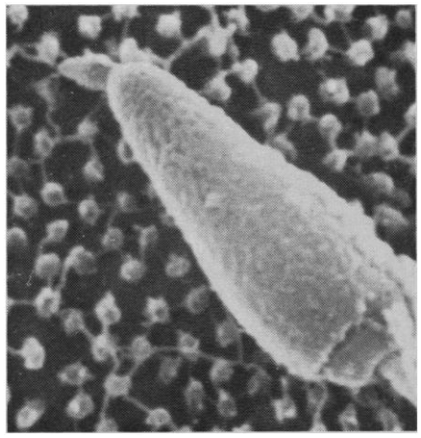

Fig. 1. Scanning electron micrograph of the head of a spermatozoon of *Strongylocentrotus purpuratus* which has undergone the acrosome reaction and attached to the vitelline surface of the egg by its acrosomal process (× 20,000).

The vitelline layer, the outer envelope of the unfertilized egg, blankets the plasma membrane surface and is a precursor of the fertilization membrane (*8, 9*). The SEM reveals that the outer surface of the vitelline layer of *S. purpuratus* eggs bears a dense array of regularly spaced projections (Fig. 1). These projections are presumably impressions of the cytoplasmic microvilli in the vitelline layer (*10*). The microvilli impressions are about 0.27 μm long and 0.16 μm in diameter, and have a center-to-center spacing of about 0.25 μm. The impressions appear to be interconnected by thin, ridge-like or strand-like structures 0.04 μm wide. These may be folds of vitelline layer material functioning as reservoirs of the extra material used in the rapid, twofold expansion in surface area at fertilization. These ridges are not seen on the surface of the fertilization membrane after its expansion is complete (see Fig. 2H).

Within 1 second after the mixing of sperm and eggs, sperm begin undergoing the acrosome reaction and attaching to the egg surface (Figs. 1 and 2A). Sperm continue to attach until about 25 seconds after sperm addition. Further stages of this sperm attachment phase can be seen in Fig. 2B (5 seconds) and Fig. 2C (15 seconds), which depict a progressive increase in the number of sperm per egg.

The acrosome reaction, triggered when the sperm contact the outer egg investments, involves the formation of the acrosomal process (*11*). This process appears to provide the major attachment between the sperm head and the surface of the egg (Fig. 1). Occasionally, fine filaments are seen attached laterally to the sperm, and these may be additionally involved in binding the sperm to the egg. It is known for the case of sperm which enter the egg that the anterior membrane of the acrosomal process fuses with the egg plasma membrane (*11, 12*). Whether the excess sperm which will be unbound during the detachment phase attach to the egg by plasma membrane fusion or by some sort of union with the vitelline layer can only be discerned with the transmission electron microscope (TEM).

The cortical reactions begin at about 25 seconds after insemination, as evidenced by the beginning of the elevation of the vitelline layer at the point of successful sperm penetration. The resultant fertilization membrane, initially "soft" and easily deformed by the mechanical stresses of fixation, hardens over the next 3 minutes (*3*). As it elevates, the fertilization membrane first appears as a smooth blister when viewed with the light microscope; however, the same area is folded and collapsed after fixation when viewed in the SEM (Fig. 2, D, E, and F). This membrane wrinkling is only seen in eggs fixed prior to completion of the hardening process. By 3 minutes after insemination, the process of fertilization membrane hardening has been completed and the fertilization membrane of zygotes fixed after that time appears smooth, round, and about half again as large as the unfertilized egg (Fig. 2G).

The detachment phase of fertilization also begins at 25 seconds after insemination, coincident with the beginning of the cortical reactions. Figure 2D illustrates an egg 30 seconds after sperm addition. The flat, circular area, to which there are no sperm attached, marks the extent of cortical granule breakdown at this time. The tail of the spermatozoon that initiated the cortical reactions can be seen emanating from a hole in the center of this transformed

area (see arrow, Fig. 2D). The cortical reactions proceed as a wave from the point of entry of the fertilizing sperm, and supernumerary sperm are unbound at the crest of this transforming wave (*13*). By 45 seconds the cortical reactions have covered half the egg (Fig. 2E); by 55 seconds they are complete and no sperm can be seen adhering to the surface of the egg (Fig. 2F) (*14*).

An enlargement of the hardened fertilization membrane at 3 minutes after insemination is shown in Fig. 2H (compare this to Fig. 1, which shows the surface of an unfertilized egg). The papillae on the fertilization membrane are what remain of the projections on the vitelline layer. Inoue and Hardy (*15*) have seen similar structures in their studies of *S. purpuratus* with the TEM. Observations of eggs in which the fertilization membrane has been ripped and partially folded back indicate that these projections are hollow. After fertilization the projections open out and shorten, their center-to-center spacing increases from 0.25 to 0.50 μm, and the interconnecting ridges or folds cannot be seen. These changes are all consistent with mechanisms of unfolding or stretching of the vitelline layer during its rapid expansion in surface area at fertilization.

The scanning electron microscope gives us an overview of fertilization not offered by any other method, a "sperm's-eye view," as well as new details about the structure of the vitelline layer. The vitelline layer of sea urchins has been very difficult to resolve with the TEM; as a consequence, those authors who could see it have attributed little structural detail to it. It can be concluded that the egg exterior visible in Fig. 1 and Fig. 2, A to C, is the vitelline layer since this layer elevates from the egg surface at fertilization. This SEM investigation shows that the vitelline layer has a definite and intricate structure, and illustrates the transformation of the vitelline layer material as it forms the template of the fertilization membrane. It is known that the contents of the cortical granules fuse with and harden the elevating vitelline layer, transforming it into the more rigid fertilization membrane (*16*). This study further demonstrates that the vitelline layer of *S. purpuratus* eggs is more than just a substratum for cortical products; the vitelline layer acts as a template which imposes its three-dimensional topography on the fertilization membrane.

That many sperm bind to the egg surface during normal fertilization is perhaps common knowledge; the sperm attachment-detachment sequence, however, has not been generally recognized. In the past, large amounts of sperm binding have been associated with the pathological condition of polyspermy induced by treatment of unfertilized eggs with nicotine or soybean trypsin inhibitor (SBTI) (*2*, *17*). These are not cases of abnormal attachment but failure of the detachment phase. Vacquier *et al.* (*2*) have shown that the detachment phase of the attachment-detachment sequence results from the action of a protease released from the

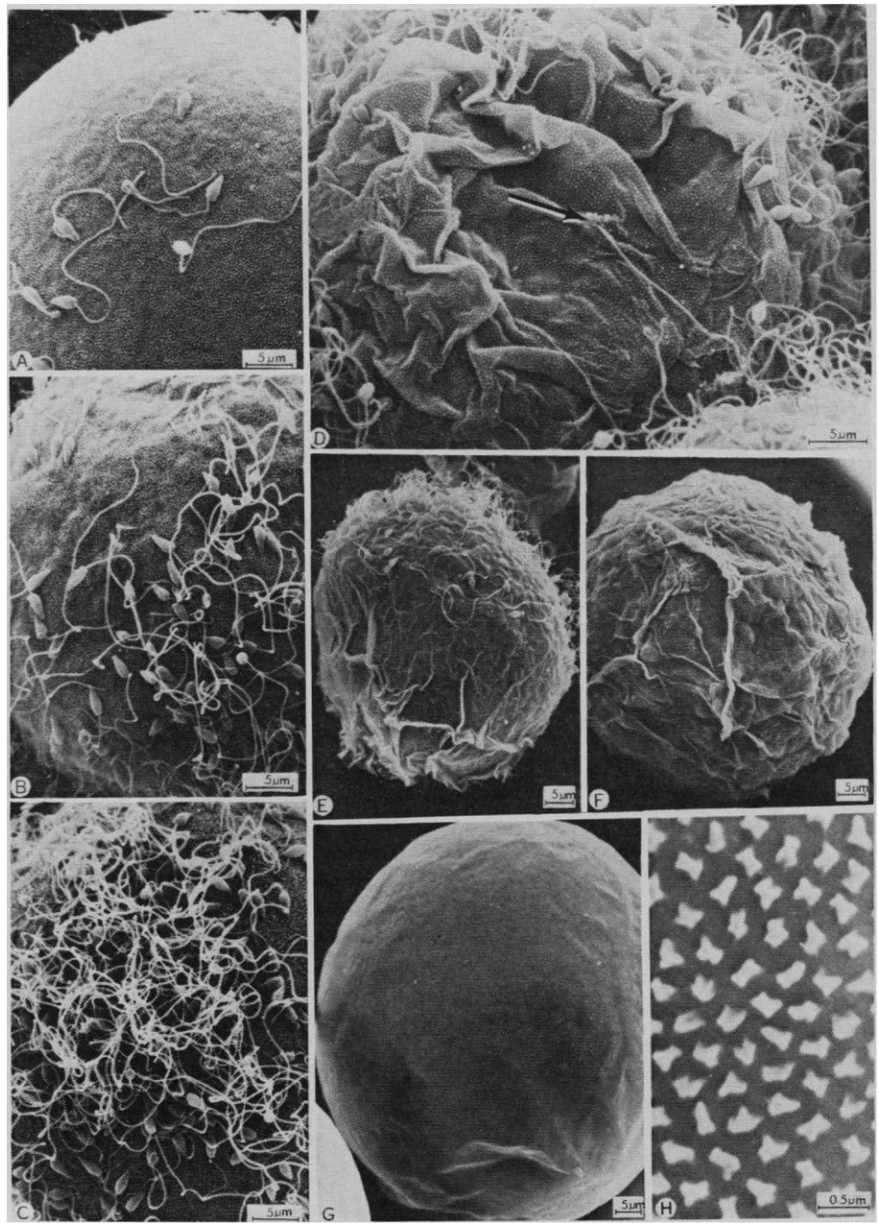

Fig. 2. Scanning electron micrographs of the sperm attachment-detachment sequence on the surface of *Strongylocentrotus purpuratus* eggs. The number of sperm bound per egg increases until 25 seconds after insemination, when the cortical reactions and the detachment sequence begins. (A) 1 second after insemination; (B) 5 seconds; (C) 15 seconds; (D) 30 seconds. The arrow points to the tail of the fertilizing spermatozoon and the hole which it made in the vitelline layer. The extent of the cortical reactions at this time is marked by the circular area from which sperm have been detached. (E) 45 seconds. Cortical granule breakdown has covered about half the egg. (F) 55 seconds. Cortical reactions are complete and all but the fertilizing sperm have been detached. (G) 3 minutes. The hardened fertilization membrane. Note that E, F, and G are at the same magnification. The differences in size and surface wrinkling are related to hardening of the fertilization membrane (see text). (H) Enlargement of G. Projections on the surface of the fertilization membrane. The eggs were fertilized at room temperature (22°C) by using 3×10^8 sperm per milliliter.

cortical granules. This protease is involved in structural alterations of the vitelline layer and aids in establishing the block to polyspermy as well as sperm detachment. Eggs fertilized in the presence of inhibitors of the protease, such as SBTI, undergo an incomplete detachment phase and become polyspermic (*2*). Nicotine induces polyspermy and also interferes with detachment (*17*). Its mechanism of action is not yet understood.

Rothschild and Swann formulated a model to explain the block against polyspermy in organisms in which fertilization is normally monospermic (*18*). From observations of the large number of sperm-egg collisions which occur during the latent period between insemination and the onset of the cortical reactions, it was realized that few collisions can be successful. Thus, Rothschild and Swann's model incorporated a factor for the probability of successful sperm-egg collision, where a successful collision is one that results in penetration of the egg cytoplasm (*18*). As shown in these micrographs, many sperm-egg collisions lead to attachment. Thus, attachment is interposed between collision and penetration, but is not a sufficient criterion for a successful penetration.

Any model explaining the block to polyspermy must therefore take into account the facts that many sperm attach to the vitelline layer and that such attachment does not necessarily lead to penetration. Ginsburg (*19*) and Paul (*20*) have suggested that the entry of supernumerary sperm may be blocked at points after the initial sperm-egg interaction. Baker and Presley (*21*), using agents that block fertilization at points prior to cortical granule breakdown, have demonstrated the existence of at least one intermediate stage in the fertilization reaction between the sperm-egg contact and the initiation of the cortical reactions.

If all sperm-egg binding sites are equivalent, our results offer strong evidence that the block to polyspermy must operate at some stage after the initial sperm-egg interaction. Such a stage could be the fusion of the plasma membranes of the sperm and egg, which has been reported to occur between 20 and 30 seconds after insemination (*22*). Another possibility is that all sperm are not physiologically equal (*23*), this inequality perhaps lying in the sperm's capacity for getting through the vitelline layer.

Steinhardt *et al.* (*24*) have demonstrated a fertilization action potential in the sea urchin egg within 3 seconds after insemination, well before cortical granule breakdown begins. This egg response to presumably the first sperm to attach to the egg may affect the quality of all further attachments; thus, the change in membrane potential may also be involved in the block to polyspermy.

Alternatively, there may be different classes of sperm binding sites on the vitelline layer. Evidence exists for the presence of at least two different classes of binding sites on the zona pellucida of golden hamster ova (*25*). If different types of sperm binding sites are present on the vitelline layer of sea urchin eggs, some of these sites may be nonfunctional in penetration. Another possibility is that different sites may admit sperm at different rates. Under conditions of simultaneous attachment of more than one sperm, the sperm bound to a site permitting the most rapid penetration could the initiate the block to polyspermy and thence exclude other sperm.

Sperm-egg interactions and blocks to polyspermy in mammals are strikingly similar to those of sea urchins. In both groups of organisms, fertilization is normally monospermic; if more than one sperm enters the egg, development is abnormal (*26*). In the hamster, many sperm also bind to the egg during the initial stages of fertilization (*25, 26*). Sperm are found bound to the zona pellucida of the hamster egg only before cortical granule breakdown. After the cortical reaction has taken place, no sperm are seen attached to the zona pellucida. As is the case in sea urchins, the hamster zona reaction, which is the transformation of the egg's exterior such that sperm no longer bind, appears to be mediated by a cortical product; treatment of eggs with cortical product before adding sperm completely inhibits binding and subsequent fertilization (*2, 26*). Although the time course of this reaction, seconds in sea urchins compared to minutes in the hamster, is quite different, the similarity in this mechanism for dealing with the prevention of polyspermy in these two widely separated animal groups is impressive.

MIA J. TEGNER
DAVID EPEL

Marine Biology Research Division, Scripps Institution of Oceanography, La Jolla, California 92037

References and Notes

1. R. D. Allen and J. L. Griffin, *Exp. Cell Res.* **15**, 163 (1958).
2. V. D. Vacquier, M. J. Tegner, D. Epel, *Nature* **240**, 352 (1972).
3. M. Paul and D. Epel, *Exp. Cell Res.* **65**, 281 (1971).
4. K. Aketa, K. Onitake, H. Tsuzuki, *ibid.* **71**, 27 (1972).
5. V. D. Vacquier, D. Epel, L. A. Douglas, *Nature* **237**, 34 (1972).
6. At this concentration of sperm we are dealing with a small, variable percentage of polyspermy, but this does not interfere with the sequence pictured here. *Strongylocentrotus purpuratus* eggs are highly resistant to polyspermy.
7. A. L. Cohen, D. P. Marlow, G. E. Garner, *J. Microsc. Paris* **7**, 331 (1968).
8. Synonyms found in the literature for our term vitelline layer are vitelline membrane, egg envelope, and primary envelope. The fertilization membrane has also been termed the activation calyx.
9. J. Runnstrom, in *Advances in Morphogenesis*, M. Abercrombie and J. Brachet, Eds. (Academic Press, New York, 1966), vol. 5, p. 221.
10. Humphreys and Lindsay present TEM pictures which show that these projections are impressions of the cytoplasmic microvilli (they use the term papillae). They also present SEM pictures of these impressions fixed differently than in this study and therefore of somewhat different dimensions [W. J. Humphreys and D. T. Lindsay, in *Proceedings of the Electron Microscopy Society of America, 29th Annual Meeting*, C. J. Arceneaux, Ed. (Claitors, Baton Rouge, La., 1971), p. 530].
11. J. C. Dan, in *Advances in Morphogenesis*, M. Abercrombie, J. Brachet, T. J. King, Eds. (Academic Press, New York, 1970), vol. 8, p. 1; C. R. Austin, *Ultrastructure of Fertilization* (Holt, Rinehart & Winston, New York, 1968), pp. 133–134.
12. A. L. Colwin and L. H. Colwin, *J. Biophys. Biochem. Cytol.* **10**, 255 (1961).
13. Membrane elevation is approximately coincident with cortical granule breakdown in *S. purpuratus* (*3*).
14. Sperm attachment as defined here is the attachment of sperm to the egg by a bond which is retained after glutaraldehyde fixation and through the various washes. Observations of living gametes occasionally show some sperm detaching more slowly from the fertilization membrane. This type of attachment is probably entrapment in egg jelly; in any event, this bond is not retained by aldehyde fixation.
15. S. Inoue and J. P. Hardy, *Exp. Cell Res.* **68**, 259 (1971).
16. Y. Endo, *ibid.* **25**, 383 (19[illegible] J. Bryan, *J. Cell Biol.* **44**, 635 (1970).
17. B. E. Hagstrom and R. D. Allen, *Exp. Cell Res.* **10**, 14 (195[illegible] F. J. Longo and E. Anderson, *J. Cell Biol.* **46**, 308 (1970).
18. L. Rothschild, *Quart. Rev. Biol.* **29**, 332 (1954).
19. A. A. Ginsburg, *Dokl. Akad. Nauk SSSR* **152**, 501 (1963).
20. M. Paul, thesis, Stanford University (1970).
21. P. F. Baker and R. Presley, *Nature* **221**, 488 (1969).
22. L. E. Franklin, *J. Cell Biol.* **25** (No. 2), 81 (1965).
23. J. Cohen, in *Advances in Comparative Physiology and Biochemistry*, O. Lowenstein, Ed. (Academic Press, New York, 1971), p. 267; H. Timourian, C. E. Hubert, R. N. Stuart, *J. Reprod. Fert.* **29**, 381 (1972).
24. R. A. Steinhardt, L. Lundin, D. Mazia, *Proc. Nat. Acad. Sci. U.S.A.* **68**, 2426 (1971); R. A. Steinhardt, S. Shen, D. Mazia, *Exp. Cell Res.* **72**, 195 (1972).
25. J. F. Hartmann and R. B. L. Gwatkin, *Nature* **234**, 479 (1971).
26. C. Barros and R. Yanagimachi, *ibid.* **233**, 268 (1970); *J. Exp. Zool.* **180**, 251 (1972).
27. This work was supported by NSF grant GB 27139 and USPHS grant 5 PO 1 HD03015-05. We thank V. D. Vacquier and N. D. Holland for critcal discussions, Ellen Flentyne and Ron La-Borde for technical help with the SEM, and Dr. W. Nierenberg for his help in obtaining the critical point apparatus.

26 June 1972; revised 27 October 1972